Analyst

Accepted Manuscript

ROYAL SOCIETY OF CHEMISTRY

www.rsc.org/analyst

GLUCOPYRANOSYL-1,4-DIHYDROPYRIDINE AS A NEW FLUORESCENT CHEMOSENSOR FOR SELECTIVE DETECTION OF 2,4,6-TRINITROPHENOL

Oran Pinrat[1], Kanokthorn Boonkitpatarakul[1], Waroton Paisuwan[2], Mongkol Sukwattanasinitt[2] and Anawat Ajavakom[2]*

[1]*Program of Petrochemistry and Polymer Science, Faculty of Science, Chulalongkorn University, Bangkok 10330, Thailand*

[2]*Nanotec-CU Center of Excellence on Food and Agriculture, Department of Chemistry, Faculty of Science, Chulalongkorn University, Bangkok 10330, Thailand*

**E-mail:anawat77@hotmail.com*

ABSTRACT

Glucopyranosyl-1,4-Dihydropyridine (Glc-DHP) was synthesized as a new fluorescent chemosensor *via* cyclotrimerization of the β-amino acrylate in the presence of $TiCl_4$. This DHP derivative is soluble in aqueous media and the solution gives a blue fluorescent signal with a quantum yield of 29%. The fluorescence signal of Glc-DHP was selectively quenched by 2,4,6-trinitrophenol (TNP) with a quenching coefficient (K_{sv}) of 4.47 x 10^4 and among the best reported detection limit of 0.94 μM. The quenching mechanism was confirmed to be the static type at low concentration region (less than 50 μM) with the significant quenching effect of competitive absorption starting from the concentration of 50 μM. Even in the real sample (seawater and industrial water), the quenching efficiencies of TNP on the fluorescence emission of Glc-DHP were proven to be at the same level with that of the test in pure water, demonstrating the practicability of the detection. Furthermore, a fluorescent paper sensor could be prepared by immersing the paper into the Glc-DHP solution. The fluorescence of the paper sensor disappeared either by writing with TNP solution or by exposure to TNP vapor. These detections could be observed by the naked eye under black light. The pH effect was proven to be a substantial factor in the quenching mechanism, providing an accurate determination of TNP, 2,4-dinitrophenol (DNP) and 4-nitrophenol (4NP) in real mixed-samples.

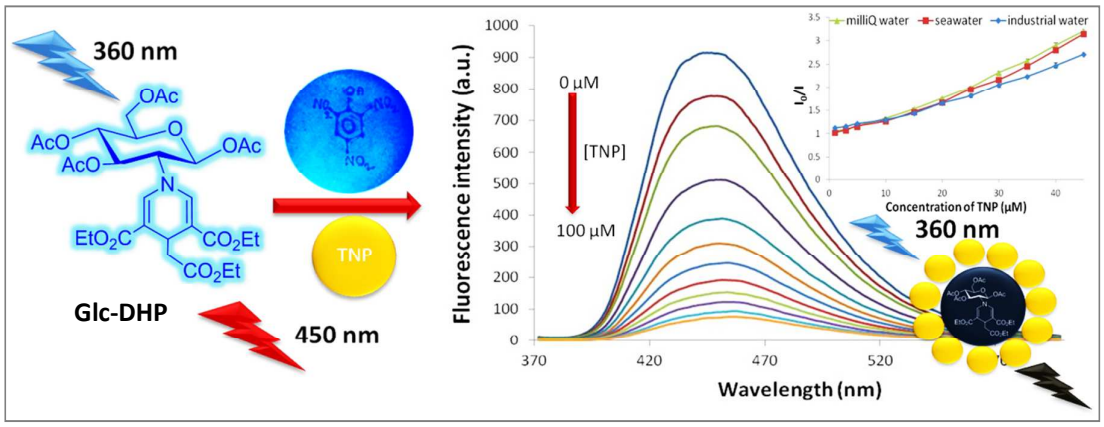

Keywords; glucosamine, fluorescent chemosensor, 1,4-dihydropyridine, nitroaromatic compound

1. Introduction

Nitroaromatic compounds (NACs), in particular 2,4,6-trinitrotoluene (TNT) and 2,4,6-trinitrophenol (TNP), are of great current concerns in both national security and environmental pollution because they are not only explosives but also recognized as toxic pollutants.[1-6] TNP is a common chemical used frequently in several organic transformations and in the leather/dye industries as a pigment. Due to its high rate of thermal expansion upon initiation with external stimuli, TNP has long been used as an important component in the manufacturing of explosives and rocket fuels. [7-10] Long time exposure to the TNP vapor can cause headaches, anemia, and toxicity to living organisms.[11,12] Thus, sensing of TNP in groundwater and seawater is highly essential for locating underwater mines and for controlling environmental pollution.[13,14] Various techniques have been developed for the detection of NACs: mass spectrometry,[15] ion mobility spectrometry,[16] electrochemical methods,[17,18] and colorimetry.[19] Compared with these analytical techniques, fluorescence-based detection offers several advantages: high sensitivity, specificity, and real-time monitoring with short response time.[20-25] Although many fluorescent sensing systems have been developed for the detection of TNT, it is not easy to differentiate the influence from TNP due to their structural similarities. Only a few examples of fluorescent sensors for selective detection of TNP via fluorescence quenching have been reported.[26-31] Interestingly, photoelectron transfer (PET) and/or energy transfer (ET) has/have been proposed as the quenching mechanism for all of the TNP sensors reported, despite the apparent overlap between the absorption band of TNP and those of the fluorophores, which strongly suggests the involvement of the competitive absorption mechanism.[32] To address the significance of the competitive absorption, the fluorescence quenching of a fluorophore with other nitrophenol (NP) derivatives should be investigated. In this work, a new glucopyranosyl-1,4-dihydropyridine (Glc-DHP) was synthesized and studied as the fluorescent compound because the 1,4-dihydropyridine (DHP) unit possesses a

similar absorption wavelength [33] to the fluorophores used in previously reported TNP sensors.[26-31] The glucopyranosyl group was incorporated to increase the water solubility of the DHP triethylester, without having to hydrolyze it to the tricarboxylic acid, as this was found to reduce its fluorescence quantum yield.[34] The systematic study of this Glc-DHP yielded a new highly sensitive TNP sensor with a capability in quantitative determination of TNP, 2,4-dinitrophenol (DNP) and 4-nitrophenol (4NP) in water samples.

2. Materials and Methods

Chemicals and materials: ethyl propiolate and $TiCl_4$ were purchased from Sigma-Aldrich and Fluka. Dichloromethane (CH_2Cl_2) was dried over CaH_2 and distilled prior to use. Thin layer chromatography (TLC) was carried out using Merck silica gel/Kieselgel 60 F254 plates with a thickness of 0.25 mm. Column chromatography was performed on Merck silica gel 60 (70-230 mesh). Nitro-containing explosives, including 2,4,6-trinitrophenol (TNP), 2,4,6-trinitritoluene (TNT), 2,4-dinitrotoluene (DNT), nitrobenzene (NB), 2-nitrobenzoic acid (NBA), benzoic acid (BA), 4-chlorobenzoic acid (CBA), 2,4-dinitrophenol (DNP), 2-nitrophenol (2NP), 3-nitrophenol (3NP), 4-nitrophenol (4NP) were of analytical grade and used direct without purification. (Caution: All nitro-containing compounds used in the present study are high explosives and should be handled only small quantities.) All other reagents were analytically pure. The seawater was collected from the gulf of Thailand, located in Rayong, Thailand, and the seawater was used without any purification. The industrial water was collected from Ban Khai industrial estate, Rayong.

Analytical Instruments: Fourier transform infrared spectrum (FTIR) was achieved from Nicolet 6700 FTIR spectrometer (Nicolet, USA). ^{1}H-NMR and ^{13}C-NMR spectra were acquired from sample solutions in $CDCl_3$, acetone-*d6*, CD_3CN, CD_3OD and DMSO-*d6* on Varian Mercury NMR spectrometer (Varian, USA) at 400 MHz and NMR spectrometer (Bruker) at 100 MHz, respectively. Absorption spectra were measured by a Varian Cary 50 UV-Vis spectrophotometer. Fluorescence spectra were performed on a Varian Cary Eclipse spectrofluorometer. The HRMS spectra were measured on an electrospray ionization mass spectrometer (microTOF, Bruker Daltonics).

2.1 Synthesis

1,3,4,6-tetra-O-acetyl-β-D-glucosamine **1**: Primary amine **1** was prepared from glucosamine hydrochloride (GlcNHCl) according to the reference method[35] in 58% yield over 4 steps. The structural data was confirmed to be in good agreement with that reported in the literature.

Ethyl β-amino acrylate **2**: To a solution of primary amine **1** (2.00 g, 5.75 mmol) in CH_2Cl_2 25.0 mL, ethyl propiolate (2.30 mL, 5.00 equiv.) was slowly added, and the reaction mixture was stirred under reflux for 3 days. The mixture was evaporated in *vacuo*, and the condensed residue was purified by column chromatography (EtOAc/Hexane = 3/7) to provide the ethyl β-amino acrylate **2** (2.10 g, 81%) as a pale yellow oil. ^{1}H NMR (400 Hz, $CDCl_3$) δ 7.62 (t, *J* = 10.8 Hz, 1H, N*H*), 6.47 (dd, *J* = 12.2, 8.3 Hz, 1H, =C*H*N), 5.56 (d, *J* = 9.2 Hz, 1H, *H*-1), 5.27 – 5.05 (m, 2H, *H*-3 and *H*-4), 4.36 (d, *J* = 8.3 Hz, 1H, C*H*=CHN), 4.30 - 4.21(m, 2H, *H*-6 and *H*-6'), 4.08 (q, *J* = 13.0, 7.2 Hz, 2H, OC*H*$_2$CH$_3$), 3.81-3.76 (m, 1H, *H*-5), 3.21 (q, *J* = 18.9, 9.5 Hz, 1H, *H*-2), 2.12 (s, 3H, Ac), 2.08 (s, 3H, Ac), 2.05 (s, 3H, Ac), 1.89 (s, 3H, Ac), 1.18 (t, *J* = 9.9 Hz, 3H, OCH$_2$C*H*$_3$). ^{13}C NMR (100 MHz, $CDCl_3$) δ 170.7, 170.2, 170.1, 169.1, 168.9, 150.3, 93.1, 85.9, 72.9, 72.6, 68.1, 62.1, 61.7, 59.2, 20.9, 20.8, 20.7, 20.6, 14.5. HRMS (ESI): M+Na$^+$, found 468.1446. $C_{19}H_{27}NNaO_{11}^+$ requires 468.1482.

1,3,4,6-tetra-O-acetyl-β-D-glucosaminyl-1,4-dihydropiridine (Glc-DHP): To the solution of ethyl β-amino acrylate **2** (2.0 g, 4.5 mmol) in dry CH_2Cl_2 25 mL in an ice bath, $TiCl_4$ (0.15 mL, 0.30 equiv.) was added rapidly and the reaction mixture was stirred overnight at room temperature under nitrogen atmosphere. After that the solution was quenched with distilled deionized water 25 mL, and the mixture was extracted with CH_2Cl_2 (3x25 mL). The organic portions were combined and neutralized by addition of 10% w/v $NaHCO_3$ solution. The organic phase was washed with deionized water (3x25 mL), dried over $MgSO_4$, and evaporated under reduced pressure. The crude product was purified by column chromatography (EtOAc/Hexane = 2/8) to provide the 1,3,4,6-tetra-*O*-acetyl-β-D-glucosaminyl-1,4-dihydropiridine (Glc-DHP) (0.38 g, 40%) as a pale yellow oil. IR: ν_{max} (neat) 2980, 2925, 1699, 1193, 1077 cm^{-1}; ^{1}H NMR (400 Hz, $CDCl_3$) δ 7.13 (d, *J* = 8.7 Hz, 2H, C*H*=C), 5.80 (d, *J* = 8.9 Hz, 1H, *H*-1), 5.40 (t, *J* = 9.5 Hz, 1H, *H*-3), 5.11 (t, *J* = 9.5 Hz, 1H, *H*-4), 4.32-4.26 (m, 1H, *H*-6), 4.23-4.06 (m, 5H, DHP-CO$_2$C*H*$_2$CH$_3$ and C*H*CH$_2$CO$_2$Et), 3.87-3.74 (m, 4H, *H*-6', *H*-5 and CH$_2$CO$_2$C*H*$_2$CH$_3$), 3.51 (t, *J* = 9.3 Hz, 1H, *H*-2), 2.48 (d, *J* = 3.3 Hz, 2H, C*H*$_2$CO$_2$Et), 2.17 (s, 3H, Ac), 2.11 (s, 3H, Ac), 2.07 (s, 3H, Ac), 1.91 (s, 3H, Ac), 1.28-1.08 (m, 9H, DHP-CO$_2$CH$_2$C*H*$_3$, CH$_2$CO$_2$CH$_2$C*H*$_3$). ^{13}C NMR (100 MHz, $CDCl_3$) δ 171.5, 170.7, 169.8, 169.6, 168.9, 166.5, 166.4, 107.8, 107.6, 100.0, 72.8, 70.4, 68.5, 65.8, 61.6, 60.5, 60.0, 39.8, 29.6, 20.9, 20.8, 20.7, 20.6, 14.5, 14.3, 1.2. HRMS (ESI): M+Na$^+$, found 664.2206. $C_{29}H_{38}NNaO_{15}^+$ requires 664.2206.

2.2 Photophysical property and fluorescence quenching study

The aqueous solution of 0.290 mM Glc-DHP (5% acetonitrile) was initially diluted to 100 μM by milliQ water to obtain a stock solution. The UV-vis absorption spectrum of the stock solution in a quartz cell with 1 cm light path was recorded from 200 to 500 nm at ambient temperature. This stock solution was further diluted to 1.00 μM by adding milliQ water for the fluorescence

measurement in a quartz cell, with a 1 cm light path recorded from 370 to 600 nm at ambient temperature using an excitation wavelength of 360 nm.

The quenching study was performed by measuring the emission spectrum of Glc-DHP (1.00 μM) mixed with an NAC (0.100 mM) in an aqueous medium. The study of pH effects on the fluorescence quenching efficiency, McIlvaine's buffers (pH 3-8), prepared from mixtures of 0.2M Na_2HPO_4 and 0.1M citric acid, were used for dilution of the stock solutions to produce the sample solutions with Glc-DHP (1.00 μM) and an nitrophenol (NP) (100 equiv.). The calibration curve for concentration determination of TNP, DNP and 4NP were obtained from the fluorescent responses at pH 3, pH 5 and pH 8.

2.3 Detection of TNP in real samples

Water to be used as media in this experiment was collected from difference sources; seawater from Pattaya, Chonburi and industrial water from the river nearby Ban Khai industrial estate, Rayong, Thailand. Water samples were used after filtration through 0.45 μm filters. The water sample (930-990 μL) in a 1.5 mL quartz cuvette with 1 cm light path was spiked with TNP solution (500 μM, 60-0 μL) and added with the Glc-DHP **1** stock solution (100 μM, 10 μL). The final solutions (1 mL) thus contained 1.0 μM Glc-DHP and 0-30 μM TNP. The fluorescence response was recorded from 370 nm to 600 nm at ambient temperature using an excitation wavelength at 360 nm.

2.4 Preparation of Glc-DHP fluorescent paper sensor

A piece of filter paper (Whatman no. 1) was immersed in a Glc-DHP solution (1.00 mM in ethanol) for 60 sec. The filter paper was then removed from the solution and air dried at room temperature for one day. To demonstrate its application as a fluorescence paper sensor, the TNP letters were written using the TNP solution (5.00 μM) onto the Glc-DHP coated filter paper. The photograph of the paper after air drying was taken under UV illumination, from a black light lamp, by a commercial digital camera.

For the TNP vapor sensing, 1.50 g of TNP powder was placed in a 3 mL vial, covered with a piece of cotton gauze and saturation with TNP vapor in the cap-closed vial was allowed overnight. Glc-DHP fluorescent paper sensor was placed on top of the opened vial with a watch glass pressing on the paper for 15 minutes. The quenching results were recorded by a commercial digital camera.

3. Results and Discussion

3.1 Synthesis of Glc-DHP

The synthesis of Glc-DHP started with the peracetylation of glucosamine by treating glucosamine hydrochloride (GlcNHCl) with *p*-anisaldehyde for NH_2 protection, followed by

acetylation using excess acetic anhydride. Removal of the *p*-methoxybenzylidine protecting group using HCl and NaOH neutralization gave the free primary amine **1** (**Figure 1**) in 58% overall yield for 4 steps.[35] The subsequent addition reaction of the primary amine **1** and ethyl propiolate afforded β-amino acrylate **2** in a good yield. Treatment of β-amino acrylate **2**, having both nucleophilic and electrophilic sites, with $TiCl_4$ resulted in the cyclotrimerization[33] to give 1,4-dihydropyridine (Glc-DHP) in 40% yield. The structure of Glc-DHP was confirmed by ^{1}H NMR, ^{13}C NMR and HR-MS.

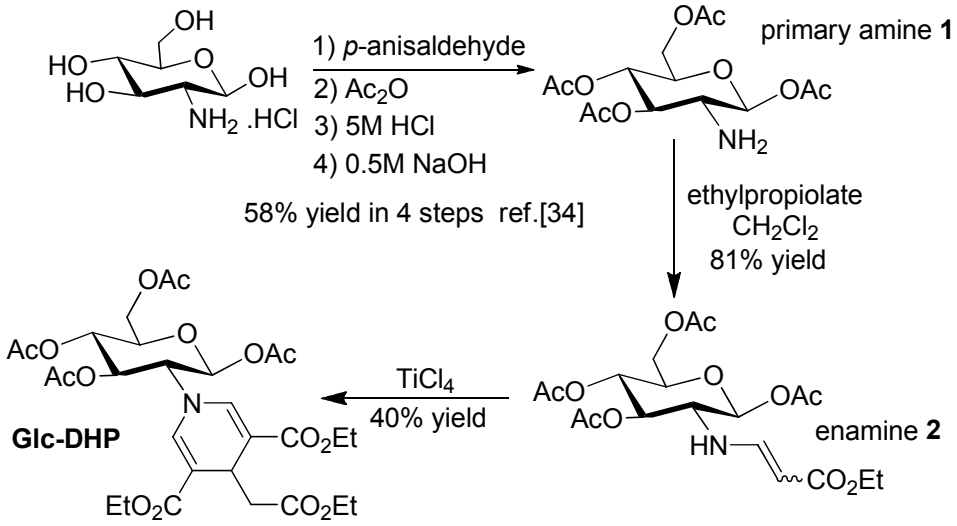

Figure 1 Synthetic scheme of Glc-DHP.

3.2 Photophysical property and fluorescence quenching study

The absorption peak of Glc-DHP in aqueous solution was observed at 360 nm with the molar absorption coefficient of 6,900 $M^{-1}cm^{-1}$ common for a 10 π-*p*-π conjugated electron system of 3,5-diester derivative of DHP chromophores.[33,36-38] Glc-DHP also exhibited a typical emission peak at 450 nm upon the excitation at 360 nm with satisfactory fluorescent quantum efficiency (Φ_f) of 0.29. To evaluate Glc-DHP as a chemosensor for the detection of NACs (TNP, TNT, DNT, NB, BA, NBA and CBA), the fluorescent responses of Glc-DHP (1 μM) towards NACs (100 equiv.) were studied in aqueous medium without pH control. Upon the addition of each NAC into the Glc-DHP solution, significant fluorescence quenching was observed only for TNP (**Figure 2**) and some quenching effects for its two derivatives, DNP and 4NP, that were observed in the interference study at higher concentration (**Figure 6**). The results suggested a possibility to use Glc-DHP as a fluorescent sensor for the selective detection and quantification of nitrophenol derivatives.

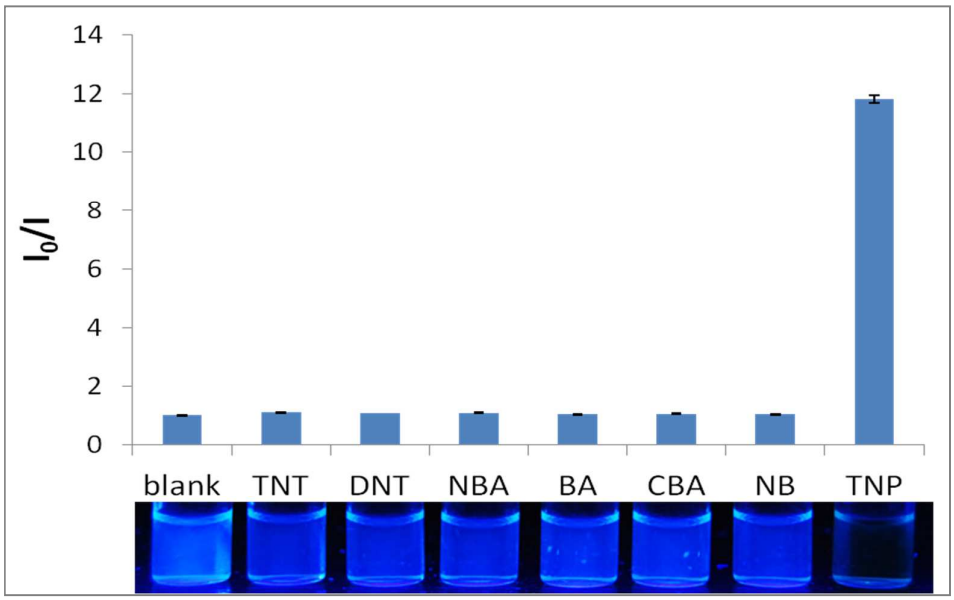

Figure 2 Fluorescence quenching ratio of Glc-DHP (1 μM) upon the addition of NAC (100 μM) in milliQ water (λ_{ex} = 360 nm).

3.3 Fluorescence titration

The fluorescence titration of Glc-DHP (1 μM) in aqueous solution toward TNP was carried out. Upon the addition of incremental amounts of TNP (1 μM to 100 μM) to the solution of Glc-DHP in aqueous solution, the quenching of fluorescence emission increased with TNP concentration (**Figure 3**). The fluorescence quenching efficiency can be represented by the Stern-Volmer constant (K_{sv}) according to the following equation;

$$\frac{I_0}{I} - 1 = K_{sv}\,[analyte]$$

A linear plot (inset **Figure 3**, blue line) gave the K_{sv} of 44,700 M^{-1} with the limit of detection (LOD) of 0.94 μM TNP, which is one of the best for the detection of TNP.[9,23,24,26,27,30] In order to understand its quenching mechanism, the temperature dependence experiment, fluorescence quenching along with the TNP titration, at the lower concentration region was conducted at the temperature of 50°C. The results showed the lower K_{sv} of 36,400 M^{-1} than that of the experiment at room temperature, implying that the quenching of this Glc-DHP with TNP is static mechanism.

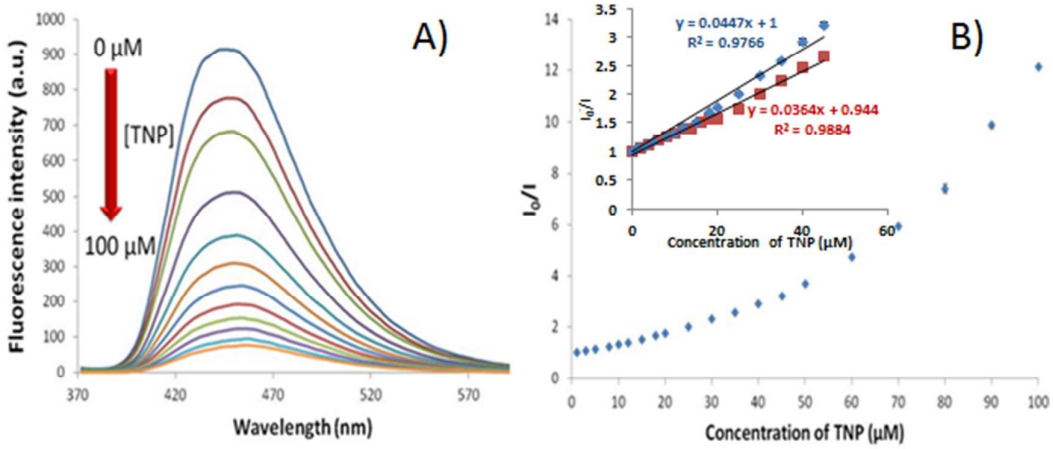

Figure 3 (a) Fluorescence quenching responses of Glc-DHP (1 µM) with the addition of TNP (0 to 100 equiv.) in aqueous solution (λ_{ex} = 360 nm) at room temperature. (b) Stern-Volmer plot in response to TNP. Inset shows the Stern-Volmer plot in the TNP concentration range of 0-45 µM at room temperature (blue line) and at 50°C (red line).

To demonstrate the utilization of Glc-DHP for determination of TNP in real water samples, the fluorescence quenching efficiencies of TNP spiked in seawater and industrial water were evaluated in comparison with that of TNP spiked in milliQ water. The three Stern-Volmer plots are nearly identical in the range of 0-30 µM (**Figure 4**), indicating insignificant interference from the matrix within the seawater and industrial water samples. However, the effect from the sample matrix became apparent at higher TNP concentrations for the industrial water samples. Therefore, the quantitative analysis of TNP in real samples should be performed at concentrations lower than 30 µM.

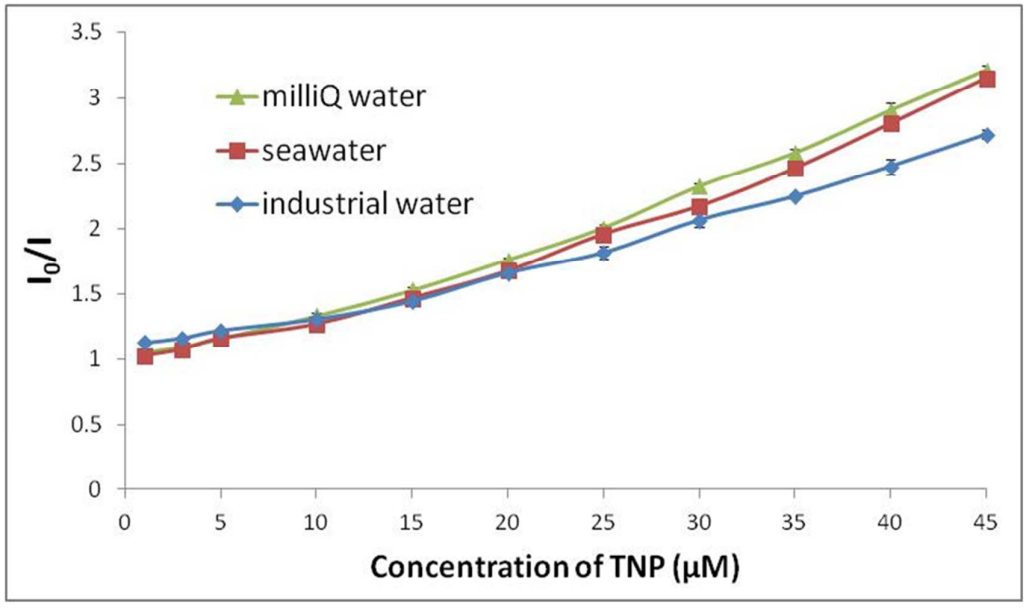

Figure 4 Stern-Volmer plots for fluorescence quenching of Glc-DHP by TNP spiked in industrial water, seawater and milliQ water.

3.5 Naked eye detection of TNP

In solution phase, the quenching of the Glc-DHP blue emission became visible at the TNP concentration of 50 μM (**Figure 5a**). Glc-DHP was also coated on a piece of filter paper from its 1 mM solution in ethanol by dipping and air-drying. When this blue fluorescent paper was stained with a seawater sample spiked with TNP (5 μM), the dark pattern of the TNP stain was clearly observed by the naked eye (**Figure 5b**). To our serendipity, this solid state detection of TNP is even more sensitive than the detection in the solution phase. This method is very convenient and rapid for the detection of TNP and should be applicable for on-site testing. The high sensitivity of the paper-based sensor may be attributed to the preconcentration effect of the sample by solvent evaporation during the detection process.

Due to its high sensitivity, it is also interesting to investigate if the Glc-DHP fluorescent paper may be used to detect TNP vapor. In a closed chamber, Glc-DHP fluorescent paper was exposed to saturated TNP vapor at 25 ºC (5.8×10^{-9} mmHg, 0.06 ppb [39,40]) for 15 minutes. After the exposure, the Glc-DHP fluorescent paper showed a clear fluorescence quenching area (**Figure 5c**). The result demonstrates that the Glc-DHP fluorescent paper can be conveniently used for the naked eye detection of saturated TNP vapor at room temperature.

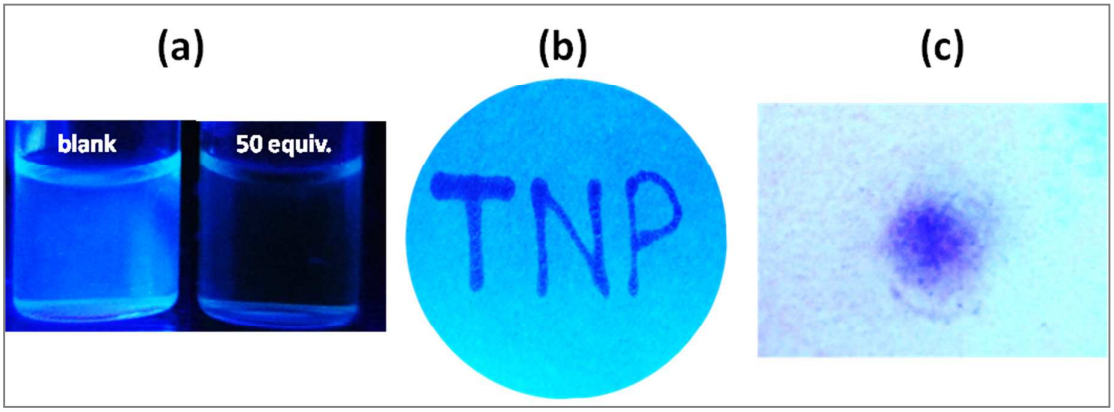

Figure 5 Visual detection of TNP with (a) 1 μM Glc-DHP in milliQ water, (b) Glc-DHP coated on paper written with seawater containing 5 μM TNP and (c) Glc-DHP coated on paper exposed to saturated TNP vapor for 15 minutes. The digital images were taken under a UV lamp.

3.6 Interference study

To further study the interference of various metal ions, NACs and NPs, we recorded the fluorescence ratio at 450 nm of Glc-DHP (1 μM) in milliQ water in the presence of 10 molar equiv. of TNP, and 50 molar equiv. of Cu^{2+}, Al^{3+}, Ba^{2+}, Ca^{2+}, Mn^{2+}, Na^{+}, Mg^{2+}, Li^{+}, K^{+}, Ag^{+}, Fe^{3+},

TNT, DNT, NB, BA, NBA, CBA, 2NP, 3NP, 4NP, and DNP (**Figure 6**). Though only little interference was observed in the case of metal cations and most NACs, there was significant interference by other NPs, especially DNP and 4NP. This type of interference by other NPs has never been reported although it is very important for the development of the TNP fluorescent chemosensor. Due to the substantial overlapping between the absorption spectra of all NPs and Glc-DHP, we suspected that the quenching mechanism involves not only the energy transfer, as suggested by all previous reports,[26-30] but also the optical filtering effect (competitive absorption).

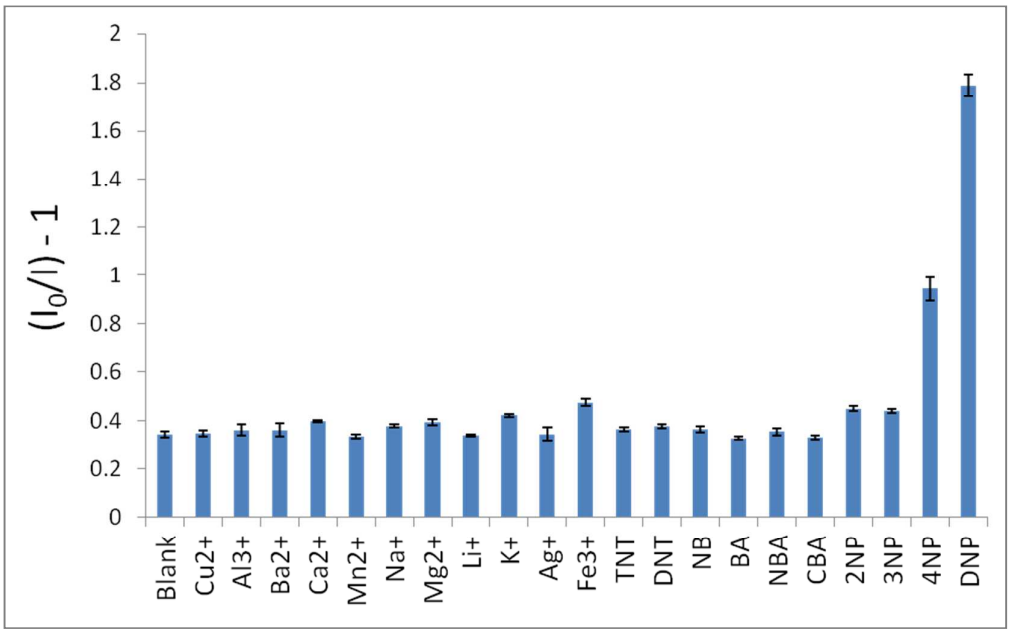

Figure 6 Fluorescence ratio at 450 nm of Glc-DHP (1 μM) in milliQ water with 10 equiv. of TNP (Blank) in the presence of 50 equiv. of Cu^{2+}, Al^{3+}, Ba^{2+}, Ca^{2+}, Mn^{2+}, Na^{+}, Mg^{2+}, Li^{+}, K^{+}, Ag^{+}, Fe^{3+}, TNT, DNT, NB, BA, NBA, CBA, 2NP, 3NP, 4NP, and DNP. (λ_{ex} = 360 nm).

3.7 Quenching mechanism

Generally, only the energy transfer from the fluorophore to TNP has been proposed as the quenching mechanism.[26-30] We also believe that this fluorescence quenching was caused predominantly by the energy transfer in the low TNP concentration region (1-20 μM), because a linear relationship was obtained in the Stern-Volmer plot in this range (**Figure 3b**). The overlap between the emission spectrum of Glc-DHP and the absorption spectrum of TNP (**Figure 7**) also supports a possible energy transfer from the excited state of Glc-DHP to TNP. The critical distance (R_0) between fluorescent donor (Glc-DHP) and acceptor (TNP) was estimated to be 2.04 nm[41] (Supporting 14),[42,43] which falls within the 2-8 nm range required for FRET, according to the Förster theory.[44,45]

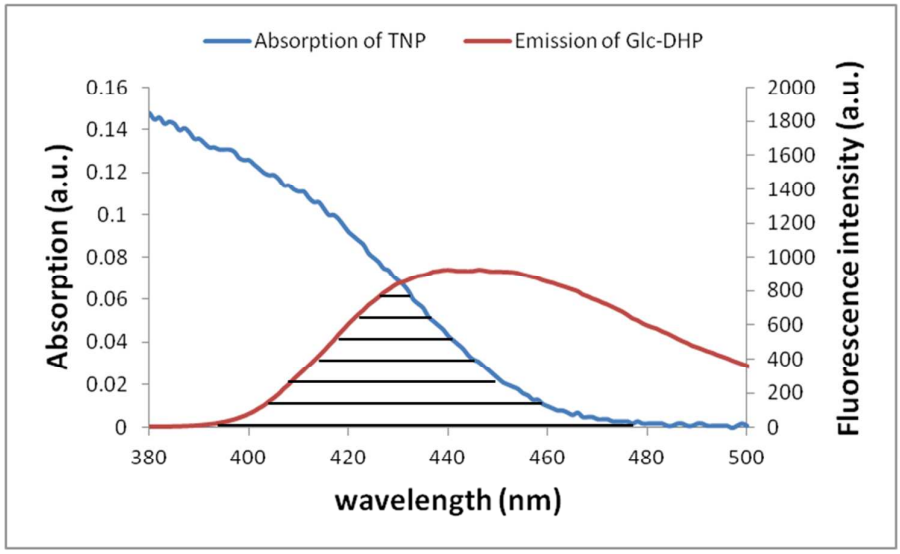

Figure 7 Spectral overlap of the absorption spectrum of TNP and the fluorescence spectrum of Glc-DHP.

The Stern-Volmer plot at higher concentration positively deviated from the linear line, which suggests that there was more than one quenching mechanism involved (**Figure 3b**). As mentioned in the previous section, competitive absorption is also another possible mechanism contributing to the fluorescent quenching effect. Table 1 shows the extinction coefficient (ε) of NPs at their λ_{max} and at 360 nm (used as the excitation wavelength) in relation to their quenching ratio (I_0/I). The data strongly indicates the possibility of competitive absorption as the quenching ratio increased with their ε values at 360 nm.

Table 1 The quenching efficiency of Glc-DHP related to the ε values of NPs at pH 8.

Compounds	Absorption			$(I_0/I) - 1$
	λ_{max} (nm)	ε at λ_{max} (M^{-1} cm^{-1})	ε at 360 nm (M^{-1} cm^{-1})	
Glc-DHP	360	6,900	6,900	-
TNP	360	12,100	12,100	6.54
DNP	360	12,000	12,000	6.01
4NP	402	15,400	7,400	2.64
3NP	256	5,500	800	0.16
2NP	415	2,100	600	0.26

All the previous experiments were carried out at pH 8 that all NPs were presumably in their phenoxide forms which should be responsible for the absorption in the range of 360-400 nm. If the pH values are lower than their pK_a, the absorption in this range should be reduced by the

protonation process turning the phenoxides to the corresponding phenols. When we performed the quenching studies at pH 3-8, the fluorescence quenchings of Glc-DHP by DNP and 4NP (pK_a = 4.2 and 7.1, respectively) decreased with the reducing pH value (**Figure 8**). The results agreed well with the formation of phenol form that has lower competitive absorption with Glc-DHP due to its low absorptivity in the Glc-DHP absorption range. However, TNP did not show any pH dependence of its quenching efficiency due to its very low pK_a of only 0.38. In the 2NP and 3NP cases (pK_a = 7.2 and 8.4, respectively), the invariance of their quenching ability by pH was due to their relatively much lower extinction coefficients comparing with TNP, DNP and 4 NP (**Table 1**). The results clearly demonstrated the relevance of competitive absorption mechanism in the quenching process and the quenching effects may be applied, with proper pH control, for the determination of TNP, DNP and 4 NP concentrations in mixed-nitrophenol derivatives.

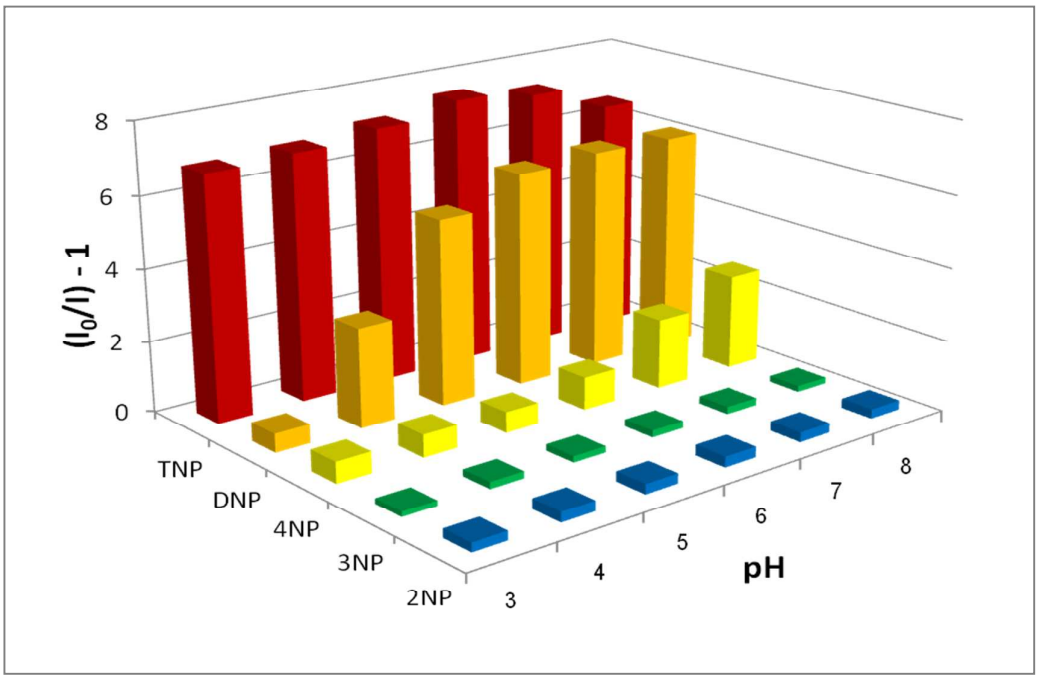

Figure 8 Fluorescence quenching profile of Glc-DHP (1 μM), after addition of each phenol derivative (100 μM) in McIlvaine's buffers at pH 3-8 (λ_{ex} = 360 nm).

Stern-Volmer plots of Glc-DHP against TNP, DNP and 4NP concentrations at pH 3, pH 5 and pH 8 provided the corresponding K_{sv} (Supporting 27). By placing these K_{sv} into eq. [1], the correlation between the quenching value (I_0/I-1) and the NP concentrations at specific pH can be obtained, as shown in eq. [2]-[4]. Therefore, each NP ratio in the real mixed samples can be estimated by carrying out the fluorescence quenching experiments at pH 3, pH 5 and pH 8 before performing calculations using eq. [2]-[4]. The percent recoveries of these samples (98-106%) (**Table 2**) clearly demonstrated that the newly developed quantification method using the Glc-DHP fluorescent sensor is highly applicable to determine each NP level in the real mixed samples.

Stern-Volmer equation for the mixed sample; where K is the slope of calibration curve.

$$\frac{I_0}{I} - 1 = K_{TNP}[TNP] + K_{DNP}[DNP] + K_{4NP}[4NP] \quad [1]$$

pH 3: $$\frac{I_0}{I} - 1 = 0.0324[TNP] + 0.0058[DNP] + 0.0054[4NP] \quad [2]$$

pH 5: $$\frac{I_0}{I} - 1 = 0.0318[TNP] + 0.0259[DNP] + 0.0062[4NP] \quad [3]$$

pH 8: $$\frac{I_0}{I} - 1 = 0.0353[TNP] + 0.0311[DNP] + 0.0207[4NP] \quad [4]$$

Table 2 Detection of mixed-nitrophenol derivatives in real water samples.

Sample	Mixed-nitrophenols	Concentration (μM)		Recovery (%)
		Actual	Calculated (mean, n = 3)	
milliQ water	TNP	10.00	9.90 ± 0.11	99.01
	DNP	10.00	10.59 ± 0.15	105.93
	4NP	10.00	10.06 ± 0.27	100.60
seawater	TNP	10.00	10.01 ± 0.29	100.18
	DNP	10.00	10.36 ± 0.57	103.62
	4NP	10.00	9.79 ± 0.11	97.97
industrial water	TNP	10.00	9.76 ± 0.06	97.66
	DNP	10.00	10.50 ± 0.07	105.01
	4NP	10.00	10.01 ± 0.35	100.10

4. Conclusion

In summary, we have reported a novel fluorescent 1,4-dihydropyridine (Glc-DHP), which can be used for the selective and sensitive detection of TNP in aqueous solution, independent of the interference of other NACs. The decrease of the fluorescence signal was proportional to the TNP concentration with a high quenching efficiency (K_{sv} = 4.47 x 10^4) providing a detection limit of 0.94 μM. In addition, a fluorescent paper sensor was fabricated for on-site convenient, sensitive and selective naked-eye detection of trace amounts of TNP either in solution or vapor down to the single digit μM level or 0.06 ppb, respectively. It was proven that the two main mechanisms were (a) energy transfer with the critical distance between Glc-DHP and TNP of 2.04 nm and (b) competitive absorption predominant from TNP concentrations of 50 μM (50 equiv.) and above. Moreover, the temperature dependence experiment at 50°C demonstrated the lower quenching efficiency (K_{sv} = 3.64 x 10^4) than that of the room temperature one referring the static quenching mechanism at concentration less than 50 μM. The pH effect was systematically proven to be a

significant factor in the quenching process, providing an accurate quantitative determination of TNP, 2,4-dinitrophenol (DNP) and 4-nitrophenol (4NP) in real water samples.

5. Acknowledgement

This study is financially supported by Nanotechnology Center (NANOTEC), NSTDA, Ministry of Science and Technology, Thailand, through its program of Center of Excellence Network. This work is part of the Project for Establishment of Comprehensive Center for Innovative Food, Health Products and Agriculture supported by the Thai Government Stimulus Package 2 (TKK2555, SP2) and the Ratchadaphiseksomphot Endowment Fund of Chulalongkorn University (RES560530126-AM).

References

(1) Singh, S. *Journal of Hazardous Materials* **2007**, *144*, 15–28.

(2) Lee, Y. H.; Liu, H.; Lee, J. Y.; Kim, S. H.; Kim, S. K.; Sessler, J. L.; Kim, Y.; Kim, J. S. *Chem. Eur. J.* **2010**, *20*, 5895 - 5901.

(3) Li, X. G.; Liao, Y.; Huang, M. R.; Strong, V.; Kaner, R. B. *Chem. Sci.* **2013**, *4*, 1970–1978.

(4) Li, D.; Liu, J.; Kwok, R. T. K.; Liang, Z.; Tang, B. Z.; Yu, J. *Chem. Commun.* **2012**, *48*, 7167–7169.

(5) Liao, Y. Z.; Strong, V.; Wang, Y.; Li, X. G.; Wang, X.; Kaner, R. B. *Adv. Funct. Mater.* **2012**, *22*, 726−735.

(6) Dey, N.; Samanta, S. K.; Bhattacharya, S. *ACS Appl. Mater. Interfaces* **2013**, *5*, 8394−8400.

(7) Toal, J. S.; Trogler C. W. *J. Mater. Chem.* **2006**, *16*, 2871–2883.

(8) Xiao, J. D.; Qiu, L. G.; Ke, F.; Yuan, Y. P.; Xu, G. S.; Wang, Y. M.; Jiang, X. *J. Mater. Chem. A* **2013**, *1*, 8745–8752.

(9) Zhou, X. H.; Li, L.; Li, H. H.; Li, A.; Yang, T.; Huang, W. *Dalton Trans.* **2013**, *42*, 12403–12409.

(10) He, G.; Peng, H.; Liu, T.; Yang, M.; Zhang, Y,; Fang, Y. *J. Mater. Chem.* **2009**, *19*, 7347–7353.

(11) Shanmugaraju, S.; Joshi, S. A.; Mukherjee, P. S. *J. Mater. Chem.* **2011**, *21*, 9130–9138.

(12) Kumar, S.; Venkatramaiah, N.; Patil, S. *J. Phys. Chem. C* **2013**, *117*, 7236−7245.

(13) Germain, M. E.; Knapp, M. *J. Chem. Soc. Rev.* **2009**, *38*, 2543-2555.

(14) Xu, B.; Wu, X.; Li, H.; Wang, L. *Macromolecules* **2011**, *44*, 5089-5092.

(15) Bader, M.; Geon, T.; Muller, J.; Angerer, J. *J. Chromatogr. B* **1998**, *710*, 91-99.

(16) Khayamian, T.; Tabrizchi, M.; Jafari, M. T. *Talanta* **2003**, *59*, 327-333.

(17) Naal, Z.; Park, J. H.; Bernhard, S.; Shapleigh, J. P.; Batt, C. A.; Abruna, H. D. *Anal. Chem.* **2002**, *74*, 140-148.

(18) Hilmi, A.; Luong, J. H. T. *Anal. Chem.* **2000**, *72*, 4677-4682.

(19) Peng, Y.; Zhang, A. J.; Dong, M.; Wang, Y. W. *Chem. Commun*. **2011**, *47*, 4505−4507.

(20) Liu, T.; Ding, L.; Zhao, K.; Wang, W.; Fang, Y. *J. Mater. Chem.* **2012**, *22*, 1069–1077.

(21) He, G.; Yan, N.; Yang, J.; Wang, H.; Ding, L.; Yin, S.; Fang, Y. *Macromolecules* **2011**, *44*, 4759–4766.

(22) Kumar, M.; Vij, V.; Bhalla, V. *Langmuir* **2012**, *28,* 12417−12421.

(23) Roy, B.; Bar, A. K.; Gole, B.; Mukherjee, P. S. *J. Org. Chem.* **2013**, *78*, 1306−1310.

(24) Liu, T.; Zhao, K.; Liu, K.; Ding, L.; Yin, S.; Fang Y. *Journal of Hazardous Materials* **2013**, *246*, 52–60.

(25) Liu, K.; Liu, T.; Chen, X.; Sun, X.; Fang, Y. *ACS Appl. Mater. Interfaces* **2013**, *5*, 9830−9836.

(26) Ma, Y.; Li, H.; Peng, S.; Kim, W. L. *Anal. Chem.* **2012**, *84*, 8415−8421.

(27) Bhalla, V.; Gupta, A.; Kumar, M. *Org. Lett.* **2012**, *14*, 3112-3115.

(28) Chan, C. Y. K.; Zhao, Z.; Lam, J. W. Y.; Liu, J.; Chen, S.; Lu, P.; Mahtab, F.; Chen, X.; Sung, H. H. Y.; Kwok, H. S.; Ma, Y.; Williams, I. D.; Wong, K. S.; Tang, B. Z. *Adv. Funct. Mater.* **2012**, *22*, 378–389.

(29) Zhao, Z.; Liu, J.; Lam, J. W. Y.; Chan, K.; Qiu, H.; Tang, Z. *Dyes and Pigments* **2011**, *91*, 258-263.

(30) Nagarkar, S. S.; Joarder, B.; Chaudhari, A. K.; Mukherjee, S.; Ghosh, S. K. *Angew. Chem. Int. Ed.* **2013**, *40,* 2104–2105.

(31) Dong, M.; Wang, Y. W.; Zhang, A. J.; Peng, Y. *Chem. Asian J.* **2013**, *8*, 1321-1330.

(32) Lohani, R. C.; Lee, K. H. *Sensors and Actuators B* **2010**, *143*, 649–654.

(33) Sirijindalert, T.; Hansuthirakul, K.; Rashatasakhon, P.; Sukwattanasinitt, M.; Ajavakom, A. *Tetrahedron* **2010**, *66*, 5161-5167.

(34) Homraruen, D.; Sirijindalert, T.; Dubas, L.; Sukwattanasinitt, M.; Ajavakom, A. *Tetrahedron* **2013**, *69*, 1617-1621.

(35) Myszka, H.; Bednarczyk, D.; Najder, M.; Kacac, W. *Carbohydrate Research* **2003**, *338*, 133-141.

(36) Chen, B.; Peng, M. L.; Wu, L. Z.; Zhang, L. P.; Tung, C. H. *Photochem. Photobiol. Sci.* **2006**, *5*, 943–947.

(37) Pa´vez, P.; Encinas, M. V. *Photochem. Photobiol.* **2007**, *83*, 722–729.

(38) Fasani, E.; Dondi, D.; Ricci, A.; Albini, A. *Photochem. Photobiol.* **2006**, *82*, 225–230.

(39) Long, Y.; Chen, H.; Wang, H.; Peng, Z.; Yang, Y.; Zhang, G.; Li, N.; Liu, F.; Pei, J. *Analytica Chimica Acta* **2012**, *744*, 82–91.

(40) Zhao, D.; Swager, T. M. *Macromolecules* **2005**, *38*, 9377-9384.

(41) Chen, T.; Zhu, S.; Cao, H.; Shang, Y.; Wang, M.; Jiang, G.; Shi, Y.; Lu, T. *Spectrochimica Acta Part A* **2011**, *78*,1295–1301.

(42) Teo, N. Y.; Kool, T. E. *Bioconjugate Chem.* **2009**, *20*, 2371–2380.

(43) Yuan, L.; Lin, W.; Zheng, K.; Zhu, S. *Accounts of Chemical Research* **2013**, *46*, 1462-1473.

(44) Yang, J. Y.; Yang, W. Y. *J. Am. Chem. Soc.* **2009**, *131*, 11644–11645.

(45) Valeur, B. New York: *Wiley Press*, **2001**.